9 SCIENTIFIC HIGHLIGHT OF THE MONTH

Half-ferromagnetism and Slater-Pauling behavior in the Heusler alloys

Iosif Galanakis*†

Institut für Festkörperforschung, Forschungszentrum Jülich, D-52425 Jülich, Germany

Abstract

The development of magnetoelectronics has increased the interest in materials which can enhance the performance of spin-dependent devices. Such materials are the so-called half-metals which present a gap in the minority band resulting in 100% spin-polarization at the Fermi level. A significant number of the intermetallic Heusler alloys have been predicted to be half-metals. In this contribution I present a complete study of both the bulk and surface properties of such Heusler alloys including both the families of the so-called half-Heusler alloys like NiMnSb and of the full-Heusler alloys like Co_2MnGe. Based on the *ab-initio* results for these compounds I discuss the origin of the gap which is fundamental for the understanding of their electronic and magnetic properties. I show that for both families of compounds the total spin magnetic moment M_t scales with the number of valence electron Z_t, such that $M_t = Z_t - 18$ for the half-Heusler and $M_t = Z_t - 24$ for the full-Heusler alloys, thus opening the way to engineer new half-ferromagnetic Heusler alloys with the desired magnetic properties. Although the surfaces loose in-general the half-ferromagnetic character and exhibit a small degree of spin-polarization, I show that in the case of compounds containing Cr, the large enhancement of the Cr moments at the surface reduces the effect of the surface states and leads to a very high spin-polarization of the surfaces, *e.g* 84% for the CrAl-terminated $Co_2CrAl(001)$ surface or even 100% for the Cr-terminated CrAs(001) surface, so that these compounds might be promising for spindependent devices.

* Young researcher within the RT-Network "Computational Magnetoelectronics". Work was performed in collaboration with Nikos Papanikolaou, University of Halle-Wittenberg, and Peter H. Dederichs, Forschungszentrum Jülich.

† E-mail address: I.Galanakis@fz-juelich.de

1. Introduction

Heusler alloys [1] have attracted during the last century a great interest due to the possibility to study in the same family of alloys a series of interesting diverse magnetic phenomena like itinerant and localized magnetism, antiferromagnetism, helimagnetism, Pauli paramagnetism or heavy-fermionic behavior [2, 3, 4, 5]. The first Heusler alloys studied were crystallizing in the $L2_1$ structure which consists of 4 fcc sublattices. Afterwards, it was discovered that it is possible to leave one of the four sublattices unoccupied ($C1_b$ structure). The latter compounds are often called half-Heusler alloys, while the $L2_1$ compounds are referred to as full-Heusler alloys. In a pioneering theory paper in 1983 de Groot and his collaborators [6] showed that one of the half-Heusler compounds, NiMnSb, is a half-ferromagnet, i.e. the minority band is semiconducting with a gap at the Fermi level E_F, leading to 100% spin polarization at E_F. Such half-ferromagnets can be considered as hybrids between metals and semiconductors. Recently the rapid development of magnetoelectronics intensified the interest on such materials since the efficiency of any spindependent device scales with the spin-polarization. Adding the spin degree of freedom to the conventional electronic devices has several advantages like nonvolatility, increased data processing speed, decreased electric power consumption and increased integration densities [7]. The current advances in new materials are promising for engineering new spintronic devices in the near future [7]. Other known half-ferromagnetic materials are *e.g.* CrO_2 [8], $La_{0.7}Sr_{0.3}MnO_3$ [8], the diluted magnetic semiconductors like (In,Mn)As [9] and very recently also CrAs in the zinc-blende structure was proposed to be a half-ferromagnet [10]. Although thin films of CrO_2 and $La_{0.7}Sr_{0.3}MnO_3$ have been verified to present practically 100% spin-polarization at the Fermi level at low temperatures [8, 11], the Heusler alloys remain attractive for technical applications like spin-injection devices [12], spin-filters [13], tunnel junctions [14], or GMR devices [15] due to their relatively high Curie temperature compared to these compounds [2].

The half-ferromagnetic character of NiMnSb in single crystals has been well-established experimentally. Infrared absorption [16] and spin-polarized positron-annihilation [17] gave a spin-polarization of ~100% at the Fermi level. Recently it has also become possible to grow high quality films of Heusler alloys, and it is mainly NiMnSb that has attracted the attention [18]. Unfortunately these films were found not to be half-ferromagnetic [8, 19, 20, 21]; a maximum value of 58% for the spin-polarization of NiMnSb was obtained by Soulen *et al.* [8]. These polarization values are consistent with a small perpendicular magnetoresistance measured for NiMnSb in a spin-valve structure [22], a superconducting tunnel junction [14] and a tunnel magnetoresistive junction [23]. Ristoiu *et al.* showed that during the growth of the NiMnSb thin films, Sb and then Mn atoms segregate to the surface, which is far from being perfect, thus decreasing the obtained spin-polarization [24]. But when they removed the excess of Sb by flash annealing, they managed to get a nearly stoichiometric ordered alloy surface being terminated by a MnSb layer, which presented a spin-polarization of about 67±9% at room temperature [24]. The temperature dependence of the spin moments for such a film was studied by Borca *et al.* [25].

Several groups have verified the half-ferromagnetic character of bulk NiMnSb using first-principles calculations [26, 27]. Larson *et al.* have shown that the actual structure of NiMnSb is the most stable with respect to an interchange of the atoms [28] and Orgassa *et al.* showed that a few percent of disorder induce states within the gap but do not destroy the half-metallicity [29]. Recently, Wijs and de Groot have shown by first-principle calculations that NiMnSb surfaces do not present 100% spin-polarization and they proposed that at some interfaces it is possible to restore the half-ferromagnetic character of NiMnSb [30]. Also recently, Jenkins and King studied by a pseudopotential technique the MnSb terminated (001) surface of NiMnSb and showed that there are two surface states at the Fermi level, which are well localized at the surface layer [31] and they persist even when the MnSb surface is covered by a Sb overlayer [32].

Webster and Ziebeck [33] and Suits [34] were the first to synthesize full-Heusler alloys containing Co and Rh, respectively. Kübler *et al.* studied the mechanisms stabilizing the ferro- or the antiferromagnetism in these compounds [35]. Ishida and collaborators have proposed that the compounds of the type Co_2MnZ, where Z stands for Si and Ge, are half-ferromagnets [36, 37]. Also the Heusler alloys of the type Fe_2MnZ have been proposed to show half-ferromagnetism [38]. But Brown *et al.* [39] using polarized neutron diffraction measurements have shown that there is a finite very small spin-down density of states (DOS) at the Fermi level instead of an absolute gap in agreement with the *ab-initio* calculations of Kübler *et al.* for the Co_2MnAl and Co_2MnSn compounds [35]. Recently, Ambrose *et al.* managed to grow a Co_2MnGe thin film on a GaAs(001) substrate by molecular beam epitaxy [40], and there also exist first-principles calculations for the (001) surface of such an alloy [41]. Finally, Geiersbach and collaborators have grown (110) thin films of Co_2MnSi, Co_2MnGe and Co_2MnSn using a metallic seed on top of a MgO(001) substrate [42].

In this contribution, I present a complete study of both the bulk and surface properties of the Heusler alloys. In total I have identified about thirty half-metallic compounds. Analyzing the *ab-initio* results using the group-theory and simple models I explain the origin of the gap in both the half- and full-Heusler alloys, which is fundamental for understanding their electronic and magnetic properties. For both families of compounds the total spin magnetic moment scales with the number of valence electron, thus opening the way to engineer new half-ferromagnetic Heusler alloys with the desired magnetic properties. Although in general the surfaces loose the half-ferromagnetic character and show only a small degree of spin-polarization, I show that in the case of compounds containing Cr, the very large Cr moments at the surface reduce the importance of the surface states and the spin-polarization of such surfaces is very high, *e.g* 84% for the CrAl-terminated $Co_2CrAl(001)$ or even 100% for the Cr-terminated CrAs(001) surface. Thus these compounds might be promising for spindependent devices.

In Section 2 I present the details of my calculations and in section 3 the electronic and magnetic properties of the XMnSb (X=Ni,Co,Rh,Pd,Ir or Pt) and Co_2MnZ (Z=Al,Si,Ga,Ge or Sn) compounds. In Section 4, I investigate the origin of the gap and the Slater-Pauling behavior. In Sections 5 and 6 I study the surface properties of the Heusler alloys and of CrAs, respectively. Finally in Section 7 I conclude and summarize my results. For a more extended presentation of the results presented in this manuscript, the reader is referred to the papers in Ref. [43].

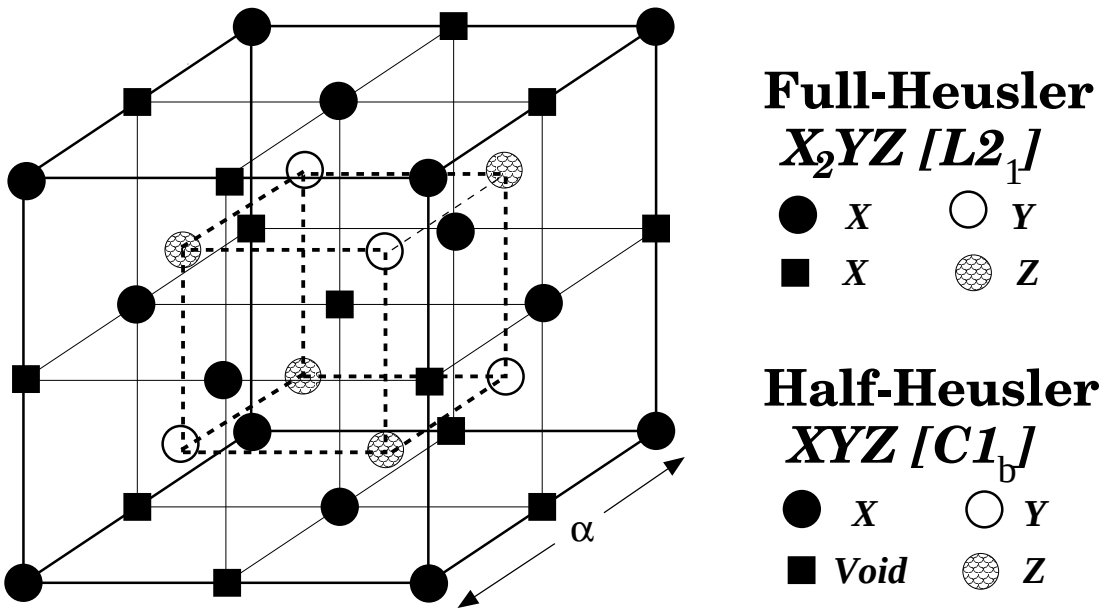

Figure 1. Schematic representation of the $C1_b$ and $L2_1$ structures. The lattice consists of 4 fcc sublattices. The unit cell is that of a fcc lattice with four atoms as basis, *e.g.* CoMnSb: Co at (0 0 0), Mn at $(\frac{1}{4}\ \frac{1}{4}\ \frac{1}{4})$, a vacant site at $(\frac{1}{2}\ \frac{1}{2}\ \frac{1}{2})$ and Sb at $(\frac{3}{4}\ \frac{3}{4}\ \frac{3}{4})$ in Wyckoff coordinates. In the case of the full Heusler alloys also the vacant site is occupied by a Co atom.

2. Computational Details

To perform the calculations, I used the Vosko, Wilk and Nusair parameterization [44] for the local density approximation (LDA) to the exchange-correlation potential [45] to solve the Kohn-Sham equations within the full-potential screened Korringa-Kohn-Rostoker (FSKKR) method [46, 47]. The full-potential is implemented by using a Voronoi construction of Wigner-Seitz polyhedra that fill the space as described in Ref. [47]. A repulsive muffin-tin potential (4 Ry high) is used as reference system to screen the free-space long-range structure constants into exponentially decaying ones [48]. For the screening I took for all the compounds interactions up to the sixth neighbors into account leading to a tight-binding (TB) cluster of 65 neighbors around each atom. To calculate the charge density, I integrated along a contour on the complex energy plane, which extends from the bottom of the band up to the Fermi level [49]. Due to the smooth behavior of the Green's functions for complex energies, only few energy points are needed; in my calculations I used 42 energy points. For the Brillouin zone (BZ) integration, special points are used as proposed by Monkhorst and Pack [50]. Only few tens of $\mathbf{k}$ are needed to sample the BZ for the complex energies, except for the energies close to the real axis near the Fermi level for which a considerably larger number of $\mathbf{k}$-points is needed. I have used a 30×30×30 $\mathbf{k}$-space grid in the full BZ to perform the integrations in the case of the bulk calculations and a two-dimensional 30×30 $\mathbf{q}_{||}$-space grid in the case of the surfaces. In addition I used a cut off of ℓ_{max}=6 for the multipole expansion of the charge density and the potential and a cut off of ℓ_{max}=3 for the wavefuctions. Finally in my calculations the core electrons are allowed to relax during the self-consistency. In all the calculations I have used the experimental lattice constants [2].

To simulate the surfaces I have used a slab with 15 metal layers embedded in half-infinite vacuum from each side. Such a slab has two equivalent surfaces avoiding the creation of slab-dipoles. This slab thickness is sufficiently large so that the layers in the middle exhibit bulk properties; they show a spin-down gap of the same width as in the bulk and the same relative position of the Fermi level and finally the magnetic moments differ less than $0.01\mu_B$ from the bulk values.

In Fig. 1, I show the $C1_b$ and $L2_1$ structures adopted by the half- and full-Heusler alloys, respectively. Both structures consist of four fcc sublattices. A half-Heusler compound has the general formula XYZ, where X is a high-valent transition metal atom, Y a lower-valent transition metal atom and Z a *sp* atom. The unit cell is that of a fcc lattice with four atoms as basis: X at (0 0 0), Y at $(\frac{1}{4}\ \frac{1}{4}\ \frac{1}{4})$, a void at $(\frac{1}{2}\ \frac{1}{2}\ \frac{1}{2})$ and the Z atom at $(\frac{3}{4}\ \frac{3}{4}\ \frac{3}{4})$ in Wyckoff coordinates. In the case of a full Heusler alloy also the void site is occupied by a X-type atom. Note that in the case of the (001) surfaces there are two different possible terminations. One contains the Y and Z type atoms while the other one contains the X atoms (and the vacant site in the case of the half-Heusler compounds).

I should also mention that the structure of the Heusler alloys is similar to the zinc-blende structure adopted by a large number of semiconductors, like GaAs, ZnSe, InAs etc, which can also be considered of consisting of four fcc sublattices. In the case of GaAs the black spheres are occupied by Ga atoms and the empty spheres by As atoms, while the other two sites are vacant. This close structural similarity should make the Heusler alloys compatible with the existing semiconductor technology and thus very attractive for industrial applications.

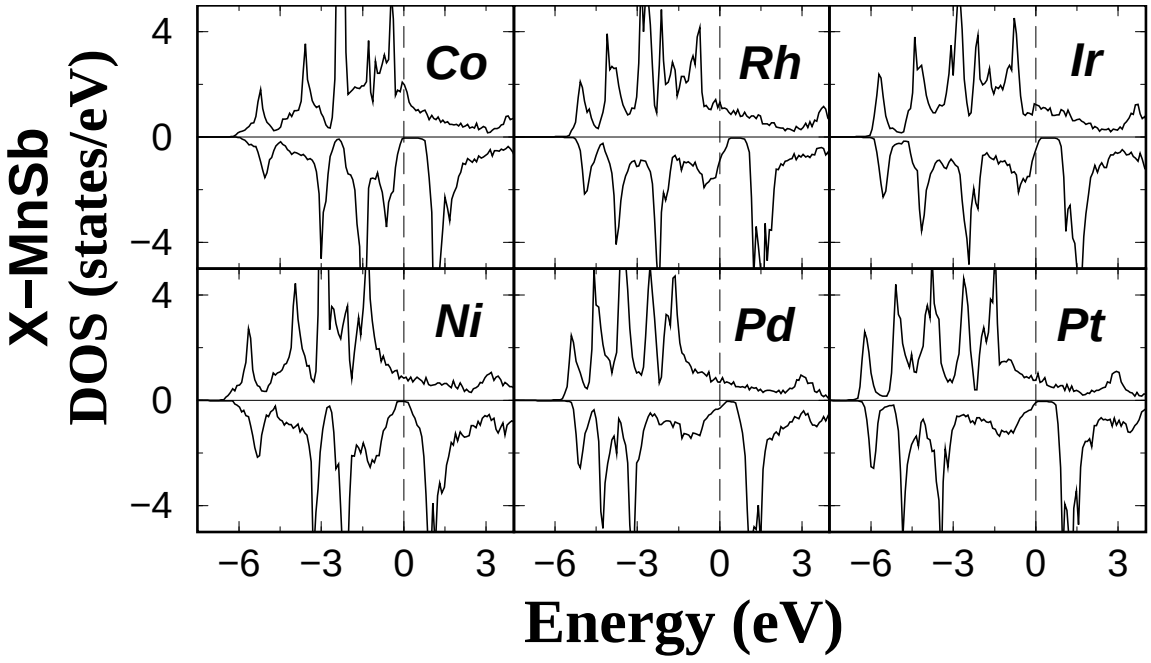

Figure 2. Spin-projected density of states for the XMnSb half-Heusler alloys. They all posses a spin-down gap but only in Co-, Ni- and Pt- based alloys the Fermi level (zero at the energy axis) falls inside the gap.

3. Electronic and Magnetic Properties

3.1 Half-Heusler alloys: X-MnSb with X= Co, Ni, Rh, Ir, Pd and Pt

Firstly I calculated the electronic structure of the half-Heusler alloys of the type XMnSb, with X being an element of the Co or Ni columns in the periodic table. These compounds are known experimentally to be ferromagnets with high Curie temperatures ranging between 500 K and 700 K for the Co, Ni, Pd and Pt compounds, while the Curie temperatures of the Ir and Rh compounds are around room temperature.[2] These compounds are known to exhibit a small disorder [2], with the exception of CoMnSb [51]. In Fig. 2 I present the spin-projected total density of states (DOS) for all the six compounds. I remark that all six compounds present a gap, which is wider in the compounds containing Co, Rh or Ir than in Ni, Pd or Pt. Sb p states occupy the lowest part of the DOS shown in the figure, while the Sb s states are located $\sim$12 eV below the Fermi level. For the Ni compound the Fermi level is at the middle of the gap and for PtMnSb at the left edge of the gap in agreement with previous full-potential linear muffin-tin orbitals method (FPLMTO) calculations on these compounds [26]. The gap in the minority NiMnSb band is about 0.5 eV wide in good agreement with the experiment of Kirillova and collaborators [16], who analyzing their infrared spectra estimated a gap width of $\sim$0.4 eV. In the case of CoMnSb the gap is considerably larger ($\sim$1 eV) than in the previous two compounds and the Fermi level is located at the left edge of the spin-down gap. CoMnSb has been studied theoretically by Kübler using the augmented spherical waves (ASW) method. He found a DOS similar to mine, with a large gap of comparable width and the Fermi level was also located at the left edge of the spin-minority gap [52]. For the other three compounds the Fermi level is located below the gap, although in the case of PdMnSb and IrMnSb it is very near the edge of the gap.

The DOS of the different systems are mainly characterized by the large exchange-splitting of the Mn d states which is around 3 eV in all cases (this is clearly seen in the atom-projected DOS of NiMnSb in Fig. 4). This large exchange splitting leads to large localized spin moments at the Mn site; the existence of the localized moments has been verified also experimentally [53]. The localization comes from the fact that although d electrons of Mn are itinerant, the spin-down electrons are almost excluded from the Mn site. In Table 1 I present the spin magnetic moments at the different sites for all the compounds under study. Here I should mention that in order to calculate the moments I integrate the spin-projected charge density inside every Wigner-Seitz polyhedron. In my calculations these polyhedra were the same for every atom. Overall the calculated moments for the Ni, Pd and Pt compounds are in very good agreement with previous *ab-initio* results [26, 27]. Experimental values for the spin-moment at the Mn site can be deduced from the experiments of Kimura *et al.* [54] by applying the sum rules to their x-ray magnetic circular dichroism spectra and the extracted moments agree nicely with my results; they found a Mn spin moment of 3.85 μ_B for NiMnSb, 3.95 μ_B for PdMnSb and 4.02 μ_B for PtMnSb. In the case of the Co-, Rh-, and IrMnSb compounds the spin magnetic moment of the X atom is

antiparallel to the Mn localized moment and the Mn moment is generally about 0.5 μ_B smaller than in the Ni, Pd and Pt compounds. The Sb atom is here again antiferromagnetically coupled to the Mn atom.

Table 1. Calculated spin magnetic moments in μ_B using the experimental lattice constants (see Ref. [2]) for the XMnSb compounds.

$m^{spin}(\mu_B)$	X	Mn	Sb	Void	Total
NiMnSb	0.264	3.705	-0.060	0.052	3.960
PdMnSb	0.080	4.010	-0.110	0.037	4.017
PtMnSb	0.092	3.889	-0.081	0.039	3.938
CoMnSb	-0.132	3.176	-0.098	0.011	2.956
RhMnSb	-0.134	3.565	-0.144	<0.001	3.287
IrMnSb	-0.192	3.332	-0.114	-0.003	3.022
FeMnSb	-0.702	2.715	-0.053	0.019	1.979

The total magnetic moment in μ_B is just the difference between the number of spin-up occupied states and the spin-down occupied states. In the half-ferromagnetic compounds all spin-down states of the valence band are occupied and thus their total number is, as in a semiconductor, an integer and the total magnetic moment is also an integer since the total valence charge is an integer. A detailed discussion of the relation between the total moment and the number of electrons will be given in Section 4. Here I notice only that the local moment per unit cell as given in Table 1 is close to 4 μ_B in the case of NiMnSb, PdMnSb and PtMnSb, which is in agreement with the half-ferromagnetic character (or nearly half-ferromagnetic character in the case of PdMnSb) observed in Fig. 2. Note that due to problems with the ℓ_{max} cutoff the KKR method can only give the correct integer number 4, if Lloyd's formula has been used in the evaluation of the integrated density of states, which is not the case in the present calculations. I also find that the local moment of Mn is not far away from the 4 μ_B although there are significant (positive) contributions from the X-atoms and a negative contribution from the Sb atom. In contrast to this I find that for the half-metallic CoMnSb and IrMnSb compounds the total moment is about 3 μ_B. Also the local moment of Mn is reduced, but only by about 0.5 μ_B. The reduction of the total moment to 3 μ_B is therefore accompanied by negative Co and Ir spin moments, *i.e* these atoms couple antiferromagnetically to the Mn moments. The hybridization between Co and Mn is considerably larger than between Ni and Mn. Therefore the minority valence band of CoMnSb has a larger Mn admixture than the one of NiMnSb whereas the minority conduction band of CoMnSb has a larger Co admixture than the Ni admixture in the NiMnSb conduction band, while the populations of the majority bands are barely changed. As a consequence, the Mn moment is reduced by the increasing hybridization, while the Co moment becomes negative, resulting finally in a reduction of the total moment from 4 to 3 μ_B. Here I should also note that further substitution of Fe for Co leads also to a half-ferromagnetic alloy with a total spin magnetic moment of 2 μ_B as has been already shown by de Groot *et al.* in Ref. [55] and by my calculations in Table 1. Finally, in the case of RhMnSb the Fermi level

is considerably below the gap and thus a part of the spin-down states are unoccupied leading to a total spin magnetic moment larger than the 3 μ_B of CoMnSb and IrMnSb.

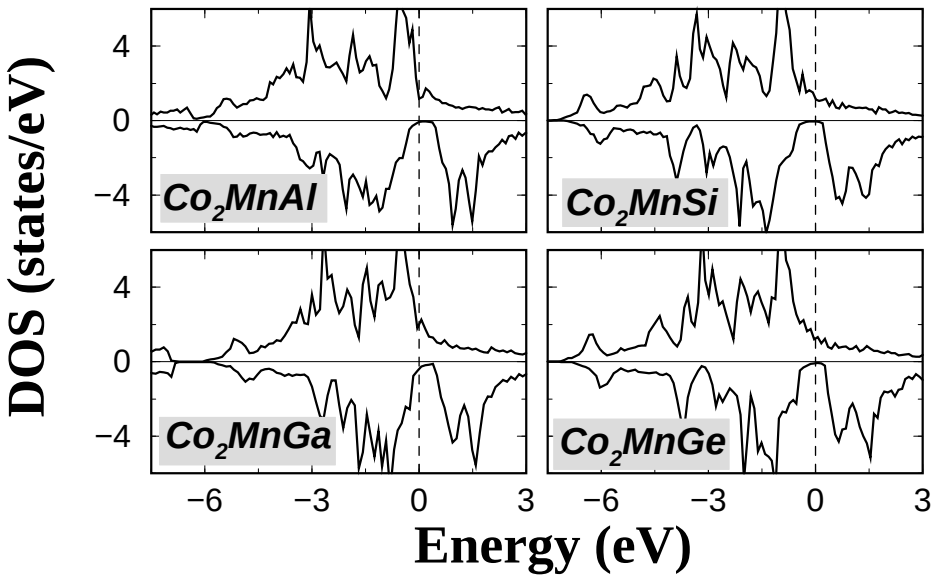

Figure 3. Calculated spin-projected DOS for the Co_2MnZ compounds, where Z stands for Al, Ga, Si and Ge. They all posses a finite very small spin-down DOS around the Fermi level.

3.2 Full-Heusler alloys: Co_2MnZ with Z= Al, Si, Ga, Ge and Sn

The second family of Heusler alloys, which I will discuss, are the full-Heusler compounds containing Co and Mn, as these are the full-Heusler alloys that have attracted most of the attention. They are all strong ferromagnets with high Curie temperatures (above 600 K) and except the Co_2MnAl they show very little disorder [2]. They adopt the $L2_1$ structure, which I present in Fig. 1. Each Mn or *sp* atom has eight Co atoms as first neighbors sitting in an octahedral symmetry position, while each Co has four Mn and four *sp* atoms as first neighbors and thus the symmetry of the crystal is reduced to the tetrahedral one. The Co atoms occupying the two different sublattices are chemically equivalent as the environment of the one sublattice is the same as the environment of the second one but rotated by 90^o. The occupancy of two fcc sublattices by Co (or in general by X) atoms distinguish the full-Heusler alloys with the $L2_1$ structure from the half-Heusler compounds with the $C1_b$ structure, like *e.g.* CoMnSb, where only one sublattice is occupied by Co atoms and the other one is empty. Although in the $L2_1$ structure, the Co atoms are sitting on second neighbor positions, their interaction is important to explain the magnetic properties of these compounds as I will show in the next section. In Fig. 3 I have gathered the spin-resolved total density of states (DOS) for the Co_2MnAl, Co_2MnGa, Co_2MnSi and Co_2MnGe compounds calculated using the FSKKR. Firstly as shown by photoemission experiments by Brown *et al.* in the case of Co_2MnSn [56] and verified by my calculations, the valence band extends 5 eV below the Fermi level and the spin-up DOS shows a large peak just below the Fermi level for these compounds. Although Ishida *et al.* [36] predicted them to be half-ferromagnets with small spin-down gaps ranging from 0.1 to 0.3 eV depending

on the material, within my calculations I find that the Fermi level falls within a region of very small spin-down DOS for all these compounds. Our results agree with the calculations of Kübler *et al.* [35] who studied the Co_2MnAl and Co_2MnSn compounds using the Augmented Spherical Wave (ASW) method and found also a very small spin-down DOS at the Fermi level and not a real gap. The reason of this pseudogap can be found in Fig. 5 where I have drawn the band structure for the minority electrons in the case of the Co_2MnGe compound. I see that the Fermi level touches the highest occupied bands at the Γ point and the lowest unoccupied bands at the K and X points and thus the indirect gap found in the half-Heusler alloys [6] is practically destroyed in these materials but there is still a reasonably large direct gap at the K and X points. However I should mention that if I considerably enlarge the figure with the band structure, it can be seen that the bands do not really touch the Fermi level but there is a very small indirect gap of the order of 0.001 eV and thus the minimum of the minority unoccupied bands at L, K and X and the maximum of the occupied bands at the Γ point are not degenerated.

In the case of the half-Heusler alloys like NiMnSb the Mn spin magnetic moment is very localized due to the exclusion of the spin-down electrons at the Mn site and amounts to about 3.7 μ_B in the case of NiMnSb. In the case of CoMnSb the increased hybridization between the Co and Mn spin-down electrons decreased the Mn spin moment to about 3.2 μ_B. In the case of the full-Heusler alloys each Mn atom has eight Co atoms as first neighbors instead of four as in CoMnSb and the above hybridization is very important decreasing even further the Mn spin moment to less than 3 μ_B except in the case of Co_2MnSn where it is comparable to the CoMnSb compound. The Co atoms are ferromagnetically coupled to the Mn spin moments and they posses a spin moment that varies from $\sim$0.7 to 1.0 μ_B, while the *sp* atom has a very small negative moment which is one order of magnitude smaller than the Co moment. The negative sign of the induced *sp* moment characterizes most of the studied full and half Heusler alloys with very few exceptions. The compounds containing Al and Ga have 28 valence electrons and the ones containing Si, Ge and Sn 29 valence electrons. The first compounds have a total spin moment of $4\mu_B$ and the second ones of 5 μ_B which agree with the experimental deduced moments of these compounds [57]. So it seems that the total spin moment, M_t, is related to the total number of valence electrons, Z_t, by the simple relation: $M_t = Z_t - 24$, while in the half-Heusler alloys the total magnetic moment is given by the relation $M_t = Z_t - 18$. In the following Section I will analyze the origin of this rule.

4. Origin of the gap and Slater-Pauling behavior

4.1 Origin of the gap: Half-Heusler alloys

In the Heusler alloys the gap basically arises from the covalent hybridization between the lower-energy *d* states of the high-valent transition metal (TM) atom like Ni or Co and the higher-energy *d* states of the lower-valent TM atom like Mn or Cr, leading to the formation of bonding and antibonding bands with a gap in between. The bonding hybrids are located mainly at the high-valent TM atom site and the unoccupied antibonding states at the lower-valent TM atom site, *e.g* in Fig. 4 the minority occupied bonding *d* states are mainly of Ni character while the unoccupied antibonding states are mainly of Mn character. Similarly to the situation of the elemental and compound semiconductors, these structures are particularly stable when only the

bonding states are occupied. In binary TM alloys this situation usually does not occur, since the total charge is too large to be accommodated in the bonding hybrids only, or, if this is possible, the covalent hybridization is not sufficient to form a gap.

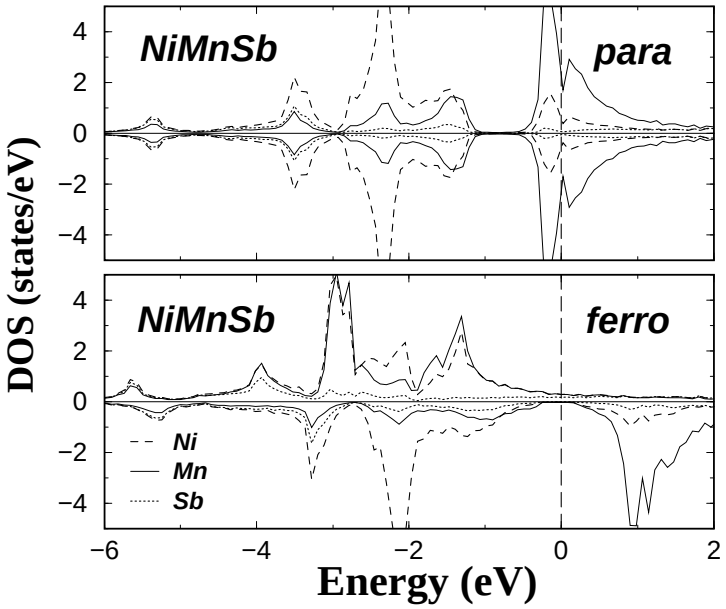

Figure 4. Ferro- and para-magnetic atomic- and spin-resolved density of states of NiMnSb. Note that the bonding d states are mainly of Ni character, while the antibonding d states are mainly of Mn character, and they are separated by a gap.

For these reasons the sp-elements like Sb play an important role for the existence of the Heusler alloys with a gap at the E_F. While an Sb atom has 5 valence electrons ($5s^2$, $5p^3$), in the NiMnSb compound each Sb atom introduces a deep lying s-band, at about -12 eV, and three p-bands below the center of the d-bands. These bands accommodate a total of 8 electrons per unit cell, so that formally Sb acts as a triple charged Sb^{-3} ion. Analogously, a Te-atom behaves in these compounds as a Te^{-2} ion and a Sn-atom as a Sn^{-4} ion. This does not mean, that locally such a large charge transfer exists. In fact, the s- and p-states strongly hybridize with the TM d-states and the charge in these bands is delocalized and locally Sb even looses about one electron. What counts is that the s- and p-bands accommodate 8 electrons per unit cell, thus effectively reducing the d-charge of the TM atoms. Since the bonding d-bands introduced above can accommodate 10 electrons, one expects therefore that the non-magnetic Heusler alloys with 18 valence electrons per unit cell are particularly stable and have a gap at E_F, i.e. are semiconducting, which requires, of course, a sufficient strong covalency between the TM partners for the gap to exist. This "18-electron rule" was recently derived by Jung *et al.* based on ionic arguments [58]. Examples for the semiconducting $C1_b$ Heusler alloys are CoTiSb and NiTiSn [59]. In the case of CoTiSb the Sb atom brings 5 valence electrons and the Co and Ti atoms 9 and 4, respectively. Of the 13 TM electrons 3 are catched by the Sb atom, so that the remaining 10 electrons just fill the bonding d-bands. In the case of NiTiSn, the Ni atom brings in one more

electron than Co, but the Sn atom with 4 valence electrons catches away 4 d-electrons, so that again 10 electrons remain for the bonding d bands.

Also for systems with more (or less) than 18 electrons, the gap can still exist. These systems are no longer semiconducting and loose part of the stability, since then also anti-bonding states are occupied (or not all bonding states are occupied). An example is the paramagnetic DOS of NiMnSb, shown in Fig. 4. Of the 22 valence electrons, four have to be accommodated in the antibonding d-bands. The high DOS at E_F signalizes that the Stoner criterium is met so that in the $C1_b$ structure NiMnSb should be a ferromagnet. Of the possible magnetic states, the half-metallic states, as shown by the spin polarized DOS of NiMnSb in Fig. 4, is particularly favored due to the gap at E_F in the minority band. Thus for these half-metallic Heusler alloys the 18-electron rule for the semiconducting Heusler is replaced by a 9-electron rule for the number of minority electrons. By denoting the total number of valence electrons by Z_t, being an integer itself, the total moment M_t per unit cell is then given by the simple rule $M_t = Z_t - 18$ in μ_B, since $Z_t - 18$ gives the number of uncompensated spins. Thus the total moment M_t is an integer quantity, assuming the values 0, 1, 2, 3, 4 and 5 if $Z_t \geq 18$. The value 0 corresponds to the semiconducting phase and the value 5 to the maximal moment when all 10 majority d-states are filled. The above relation naturally explains why *e.g.* NiMnSb with $Z_t = 22$ has a total moment of 4 μ_B, CoMnSb with $Z_t = 21$ a moment of 3 μ_B and FeMnSb with $Z_t = 20$ a moment of 2 μ_B.

4.2 Origin of the gap: Full-Heusler alloys

As I mentioned above in section 3.2, the total spin magnetic moments of the Co_2MnZ compounds follow the $M_t = Z_t - 24$ rule. Similarly to the above discussion on the half-Heusler alloys this rule means that there are 12 occupied spin-down states, as the total moment, which is the number of uncompensated spins, is given by the total number of valence electrons Z_t minus two times the number of minority electrons. It is important in order to explain the properties of these compounds to take into account firstly the interactions between the two inequivalent Co sites and then their interaction with the Mn or the sp atom (see Fig. 5a), as was also the case for the Fe_2MnZ compounds [38]. Firstly, similar to the half-Heusler alloys the sp atom creates one s band and three p bands which are fully occupied. The s electrons transform following the Γ_1 representation; I do not show this band in Fig. 5b as it very low in energy and is well separated by the other bands. The p electrons of the sp atom transform following the Γ_{15} representation and they hybridize with p electrons of the Mn and of the Co that transform with the same representation. As can be seen in the band structure, these bands are lower than the bands that have mainly d character but they are not well separated by them (there is a band crossing along the ΓK direction). As in the half-Heusler alloys, the 4 sp bands can be only partially filled by the n valence electrons of the sp atom ($n = 3$ for Al, Ga or 4 for Si Ge and Sn), so that an additional $8 - n$ d electrons are accommodated in these bands (4 d-electrons in the case of Co_2MnGe or 5 d-electrons for Co_2MnAl). Therefore in both kind of Heusler alloys the effective number of d electrons (in the higher lying d bands) can be controlled by the valence of the sp atom. This is a very unusual behavior for metallic systems, which can be used to engineer Heusler alloys with very different magnetic properties (see next section). Before going on discussing the behavior of the d orbitals we should note that the band structure seems to be symmetric along the LΓ and

KX directions due to the backfolding of the bands caused by the two Co atoms per unit cell.

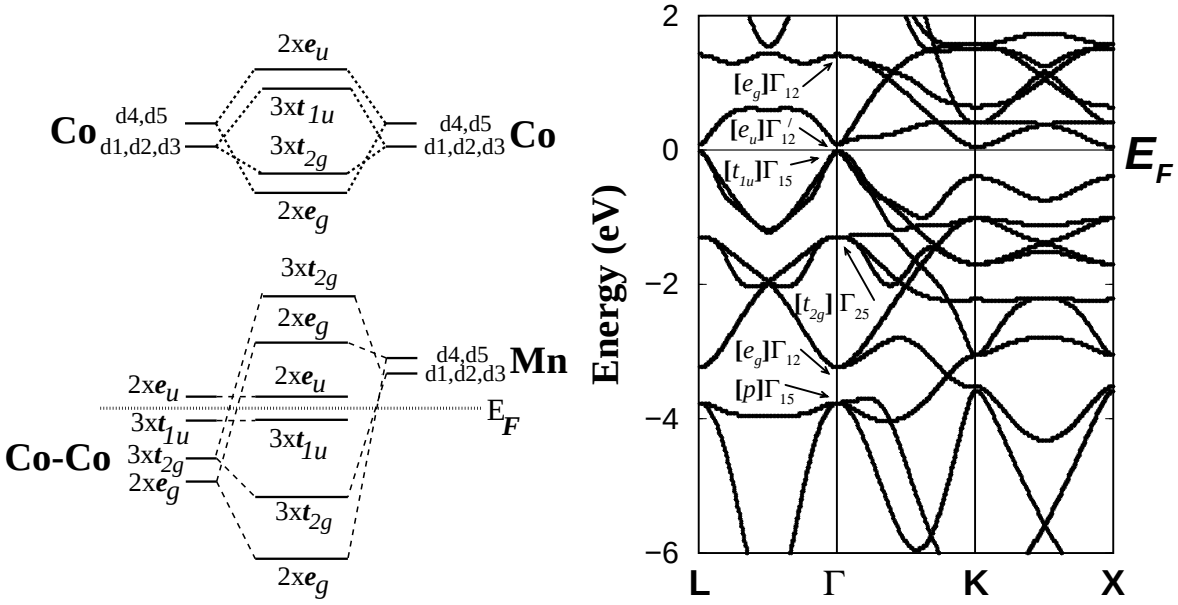

Figure 5. (a)Possible hybridizations between spin-down orbitals sitting at different sites in the case of the Co_2MnGe compound. To explain the properties of the full Heusler alloys, firstly I consider the hybridization between the two different Co atoms and afterwards the hybridization with the Mn atom. The coefficient represents the degeneracy of each orbital. (b) Spin-down band structure of the Co_2MnGe compound. The indirect gap, present in the half-Heusler alloys, is practically destroyed. In brackets I present the type of orbitals transforming following each representation.

In the case of the half-Heusler alloys, like CoMnSb, there is only one Co atom per unit cell and its d valence electrons are hybridizing with the Mn ones creating five bonding states below the Fermi level and five antibonding ones above the Fermi level. In the full-Heusler alloys the existence of the second Co atom makes the physics of these systems more complex. In order to discuss the behavior of the d electrons in the full Heusler alloys I have drawn schematically in Fig. 5a the possible hybridizations between the different atoms. The $d_{1...5}$ orbitals correspond to the d_{xy}, d_{yz}, d_{zx}, $d_{3z^2-r^2}$ and $d_{x^2-y^2}$ orbitals, respectively. The symbol e_g means that the orbital transform following the E_g representation and in the band structure I also present the representations of the symmetry group of the Γ point that has been introduced in Ref. [60]. Note that due to symmetry, the e_g orbitals at the Co site can only couple with e_g orbitals at the other Co site or at the Mn site. The same applies for the t_{2g} orbitals. Looking at Fig. 5a I see firstly that when two neighboring Co atoms interact, their d_4 and d_5 orbitals form bonding e_g and antibonding e_u states (the coefficient in front of each orbital is the degeneracy of this orbital). The d_1, d_2 and d_3 orbitals of each Co also hybridize creating a triple degenerated bonding t_{2g} orbital and a triple degenerated antibonding t_{1u} orbital. As mentioned above the $L2_1$ structure obeys the tetrahedral symmetry T_d but if only the Co sites are considered, they form a cubic lattice obeying the octahedral symmetry O_h. The e_u and t_{1u} hybrids obey the higher O_h symmetry and for symmetry reasons they cannot couple to either the d states of the Mn nor the d states of the Ge atoms.

As I show in the second part of Fig. 5a, the double degenerated e_g orbitals hybridize with the d_4 and d_5 of the Mn that transform also with the same representation. They create a double degenerated bonding e_g state that is very low in energy and an antibonding one that is unoccupied and above the Fermi level. The $3 \times t_{2g}$ Co orbitals couple to the $d_{1,2,3}$ of the Mn and create 6 new orbitals, 3 of which are bonding and are occupied and the other three are antibonding and high in energy. Finally the $2 \times e_u$ and $3 \times t_{1u}$ Co orbitals cannot couple with any of the Mn d orbitals as there are none transforming with the u representations. With respect to the Mn and the Ge atoms these states are therefore non-bonding. The t_{1u} states are below the Fermi level and they are occupied while the e_u are just above the Fermi level. Thus in total 8 minority d bands are filled and 7 are empty. Our description is somewhat different from the one in Ref. [38] where it has been assumed that the orbitals just below the Fermi level are also t_{2g} and not t_{1u} as in my case. To elucidate this difference I have drawn in Fig. 6 the atomic-resolved d DOS projected on the double degenerated and the triple degenerated representations. Although I cannot distinguish in my projection the t_{2g} from the t_{1u} and the e_g from the e_u, around the Fermi level the Mn atom presents a broad spin-down gap which is not present at the Co sites. So the minority states around the gap are localized at the Co and do not couple to Mn, and the only states that have this property are the t_{1u} and the e_u. Thus the peak below the Fermi level is the $3 \times t_{1u}$ state and the peak just above the Fermi level is the $2 \times e_u$ state. This also explains why the gap is small. The two Cobalt atoms are second neighbors and their hybridization is not so strong and the splitting of the states is small and thus the energy distance between the t_{1u} levels and the e_u ones is small. As these states do not hybridize with the Mn states their splitting does not change and the gap is considerably smaller than the one in the half-Heusler alloys. In the latter compounds I have only one Co atom per unit cell coupling to the Mn atom and so the t_{1u} and the e_u states are absent and only the e_g and t_{2g} survive. Therefore a large gap exists in the half-Heusler alloys and the minority valence bands contain 9 electrons: $1 \times s$, $3 \times p$ and $5 \times d$.

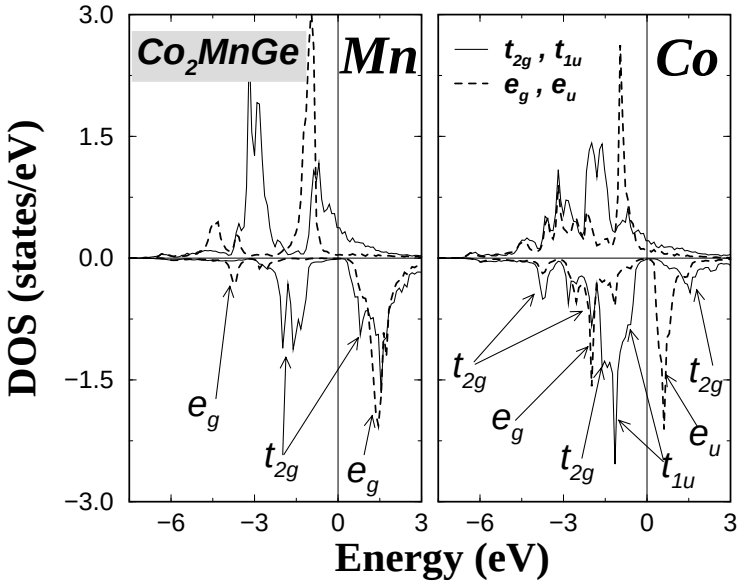

Figure 6. Projected d DOS on the double and on the triple degenerated representations for each atom in the Co_2MnGe compound. I also give the character of each peak for the spin-down states. Notice that

in the minority bands around the Fermi level there are only Co states.

To summarize, in the case of the full-Heusler alloys I have 8 occupied minority d states per unit cell: the double degenerated e_g very low in energy, the triple degenerated t_{2g} orbital and finally the triple degenerated t_{1u} just below the Fermi level. Thus in total I have 12 minority occupied states per unit cell, one with s character, three with p character and 8 with d character. Therefore the total moment obeys the simple rule $M_t = Z_t - 24$, as compared to $M_t = Z_t - 18$ for the half-Heusler alloys. Note here that as shown in Fig. 5a I have in total 15 spin-down d states, meaning 30 in total if I take into account both spin directions, so the states count is correct as each of the two Co atoms and the Mn one contributes totally 10 d states. I can trace these states also in the spin-down band structure analyzing the character of each band at the Γ point. Firstly as said above I have a s like band not shown in Fig. 5b with a Γ_1 state at the Γ point and then I find at Γ a triple degenerated point that has the Γ_{15} representation corresponding to the p like orbitals. Above this point there is a double-degenerated Γ_{12} point which corresponds to the e_g orbitals while the other e_g orbitals for Co_2MnGe are found above the Fermi level and also above the unoccupied e_u orbitals that correspond to the double degenerated point with the Γ'_{12} symmetry. Finally, there are two triple degenerated points Γ_{25} and Γ_{15} which correspond to the occupied t_{2g} and t_{1u} orbitals, respectively, while the other unoccupied t_{2g} orbitals (Γ_{25}) are high in energy and are not shown in the figure.

From the above discussion I find that in the minority band 7 d states above E_F are unoccupied. Thus the largest possible moment, which a full-Heusler alloys can have, is 7 μ_B, since in this case all majority d states are filled. This is different from the half-Heusler compounds which have five empty d-states in the minority band and therefore a maximum moment of 5 μ_B.

4.3 Slater-Pauling Behavior

As I discussed in Section 4.1 both the half- and the full-Heusler compounds follow the well-known later-Pauling behavior for the binary transition metal (TM) alloys [52]. In such a picture the total spin moment M_t scales with the total number of valence electrons Z_t. The difference between the different alloys is that in the Heusler alloys the TM minority population is fixed at 5 or 8 for the half and full alloys, respectively, and the screening is achieved by filling the majority band, while in the binary TM alloys the majority band is filled and the charge neutrality is achieved by filling the minority states. As a result, for the Heusler alloys the moment increases with the total charge Z_t, while in the TM binary alloys it decreases with increasing Z_t, since the total moment is given by $M_t = 10 - Z_t$.

In Fig. 7 I have gathered the calculated total spin magnetic moments for the half-Heusler alloys I studied as a function of the total number of valence electrons. With dashed line I represent the rule $M_t = Z_t - 18$ obeyed by these compounds. In such a picture the total moment M_t is an integer quantity, assuming the values 0, 1, 2, 3, 4 and 5 if $Z_t \geq 18$. The value 0 corresponds

to the semiconducting phase and the value 5 to the maximal moment when all 10 majority d-states are filled. Firstly I varied the valence of the lower-valent (*i.e.* magnetic) transition metal atom. Thus I substitute V, Cr and Fe for Mn in the NiMnSb and CoMnSb compounds using the experimental lattice constants of the two Mn compounds. For all these compounds I find that the total spin moment scales accurately with the total charge and they all present the half-ferromagnetism.

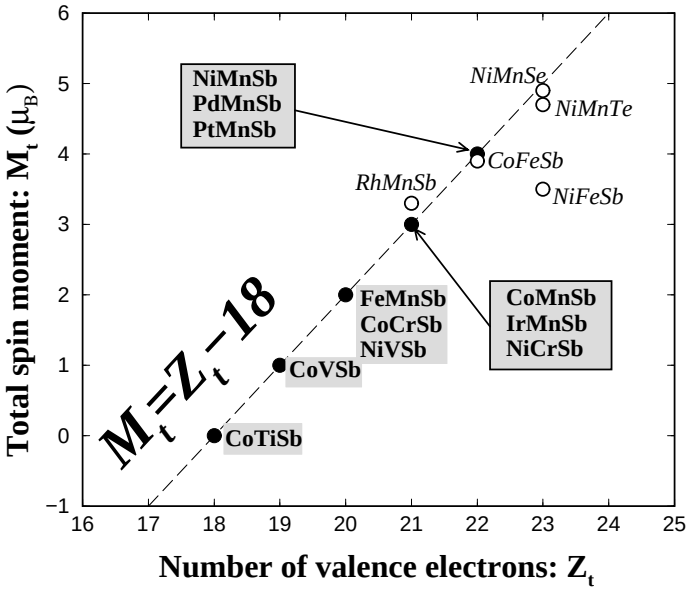

Figure 7. Calculated total spin moments for all the studied half Heusler alloys. The dashed line represents the Slater-Pauling behavior. With open circles we present the compounds deviating from the SP curve.

As a next test I have substituted Fe for Mn in CoMnSb and NiMnSb, but both CoFeSb and NiFeSb loose their half-ferromagnetic character. In the case of NiFeSb the majority d-states are already fully occupied as in NiMnSb, thus the additional electron has to be screened by the minority d-states, so that the Fermi level falls into the minority Fe states and the half-metallicity is lost; for half-metallicity a total moment of 5 μ_B would be required which is clearly not possible. For CoFeSb the situation is more delicate. This system has 22 valence electrons and if it would be a half-ferromagnet it should have a total spin-moment of 4 μ_B like NiMnSb. In reality my calculations indicate that the Fermi level is slightly above the gap and the total spin-moment is slightly smaller than 4 μ_B. The Fe atom possesses a comparable spin-moment in both NiFeSb and CoFeSb compounds contrary to the behavior of the V, Cr and Mn atoms. Except NiFeSb other possible compounds with 23 valence electrons are NiMnTe and NiMnSe. I have calculated their magnetic properties using the lattice constant of NiMnSb. As shown in Fig.7, NiMnSe almost makes the 5 μ_B (its total spin moment is 4.86 μ_B) and it is nearly half-metallic. NiMnSe as was also the case for NiMnAs shows big changes in the majority band compared to NiMnSb or NiMnTe, since antibonding p-d states, which are usually above E_F, are shifted below the Fermi level, thus increasing the total moment to nearly 5 μ_B.

Following the discussion of the previous section I will go on investigating the Slater-Pauling behavior of the full-Heusler alloys and in Fig. 8 I have plotted the total spin magnetic moments for all the compounds under study as a function of the total number of valence electrons. The dashed line represents the rule: $M_t = Z_t - 24$. In the following I will analyze some of these results. Overall I see that many of my results coincide with the Slater-Pauling curve. Some of the Rh compounds show small deviations which are more serious for the Co_2TiAl compound. I see that there is no compound with a total spin moment of 7 μ_B or even 6 μ_B. Moreover I found also examples of half-metallic materials with less than 24 electrons, Mn_2VGe with 23 valence electrons and Mn_2VAl with 22 valence electrons. Firstly, I have calculated the spin moments of the compounds Co_2YAl where Y= Ti, V, Cr, Mn and Fe. The compounds containing V, Cr and Mn show a similar behavior. As I substitute Cr for Mn, that has one valence electron less than Mn, I depopulate one Mn spin-up state and thus the spin moment of Cr is around 1 μ_B smaller than the Mn one while the Co moments are practically the same for both compounds. Substituting V for Cr has a larger effect since also the Co spin-up DOS changes slightly and the Co magnetic moment is increased by about 0.1 μ_B compared to the other two compounds and V possesses a small moment of 0.2 μ_B. This change in the behavior is due to the smaller hybridization between the Co atoms and the V compared to the Cr and Mn atoms. Although all three Co_2VAl, Co_2CrAl and Co_2MnAl compounds are on the SP curve as can be seen in Fig. 8, this is not the case for the compounds containing Fe and Ti. If the substitution of Fe for Mn followed the same logic as the one of Cr for Mn then the Fe moment should be around 3.5 μ_B which is a very large moment for the Fe site. Therefore it is energetically more favorable for the system that also the Co moment is increased, as it was also the case for the other systems with 29 electrons like Co_2MnSi, but while the latter one makes it to 5 μ_B, Co_2FeAl reaches a value of 4.9 μ_B. In the case of Co_2TiAl, is is energetically more favorable to have a weak ferromagnet than an integer moment of 1 μ_B as it is very difficult to magnetize the Ti atom. Even in the case of the Co_2TiSn the calculated total spin magnetic moment of 1.78 μ_B (compared to the experimental value of 1.96 μ_B [61]) arises only from the Co atoms as was also shown experimentally by Pendl *et al.* [62], and the Ti atom is practically paramagnetic and the latter compound fails to follow the SP curve.

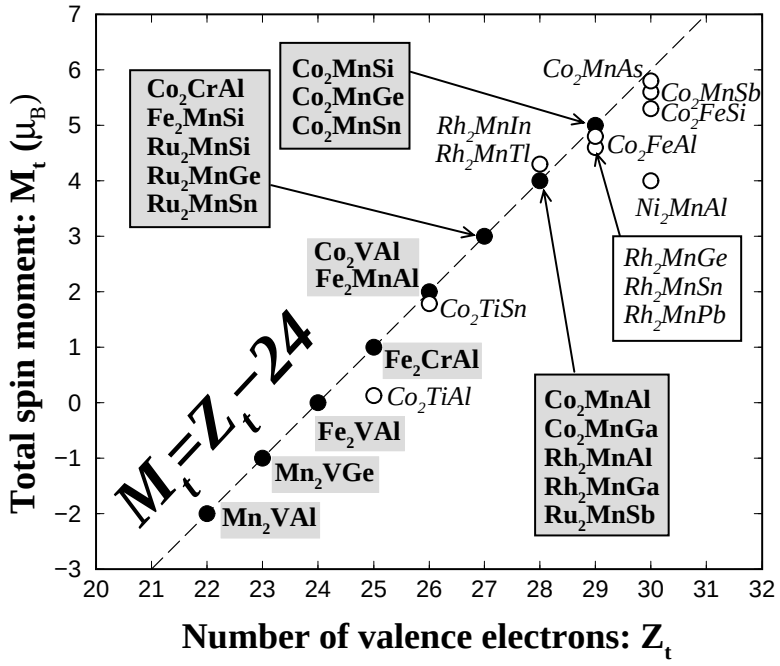

Figure 8. Calculated total spin moments for all the studied full Heusler alloys. The dashed line represents the Slater-Pauling behavior. With open circles we present the compounds deviating from the SP curve.

As a second family of materials I have calculated also the compounds containing Fe. Fe_2VAl has in total 24 valence electrons and is a semimetal, *i.e.* paramagnetic with a very small DOS at the Fermi level, as it is already known experimentally [63]. All the studied Fe compounds follow the SP behavior as can be seen in Fig. 8. In the case of the Fe_2CrAl and Fe_2MnAl compounds the Cr and Mn atoms have spin moments comparable to the Co compounds and similar DOS. In order to follow the SP curve the Fe in Fe_2CrAl is practically paramagnetic while in Fe_2MnAl it has a small negative moment. When I substitute Si for Al in Fe_2MnAl, the extra electron exclusively populates Fe spin-up states and the spin moment of each Fe atom is increased by 0.5 μ_B contrary to the corresponding Co compounds where also the Mn spin moment was considerably increased. Finally I calculated as a test Mn_2VAl and Mn_2VGe that have 22 and 23 valence electrons, respectively, to see if I can reproduce the SP behavior not only for compounds with more than 24, but also for compounds with less than 24 electrons. As I have already shown Fe_2VAl is paramagnetic and Co_2VAl, which has two electrons more, has a spin moment of 2 μ_B. Mn_2VAl has two valence electrons less than Fe_2VAl and its total spin moment is $-2\,\mu_B$ and thus it follows the SP behavior. To my knowledge there is no compound with 23 valence electrons, which has been studied experimentally, so I decided to calculate Mn_2VGe using the lattice constant of Mn_2VAl. I found that adding one electron to Mn_2VAl results in a decrease of the absolute value of both the Mn and V spin moments (note that V and Mn are antiferromagnetically coupled) so that the resulting Mn_2VGe total spin magnetic moment is -1 μ_B following the SP curve as can be also seen in Fig. 8.

To investigate further the Slater-Pauling behavior of the full-Heusler alloys I studied the ones containing a $4d$ transition metal atom. The Ru compounds are antiferromagnets with Néel temperatures that reach room temperature [64]. I have calculated their properties assuming that they are ferromagnets. Contrary to the Ru compound which follow the SP curve, in the case of the Rh ones [34, 65] only Rh_2MnAl and Rh_2MnGa are exactly on the SP curve. The rest of them present small deviations.

As I have already mentioned the maximal moment of a full-Heusler alloy is seven μ_B, and should occur, when all 15 majority d states are occupied. Analogously for a half-Heusler alloy the maximal moment is 5 μ_B. However this limit is difficult to achieve, since due to the hybridization of the d states with empty sp-states of the transition metal atoms (sites X and Y in Fig. 1), d-intensity is transferred into states high above E_F, which are very difficult to occupy. Although in the case of half-Heusler alloys, I could identify systems with a moment of nearly 5 μ_B, the hybridization is much stronger in the full-Heusler alloys so that a total moment of 7 μ_B seems to be impossible. Therefore I restrict my search to possible systems with 6 μ_B, *i.e.* systems with 30 valence electrons, but as shown also in Fig. 8, none of them makes exactly the 6 μ_B. Co_2MnAs shows the largest spin moment: 5.8 μ_B. If I increase its lattice constant by 3% the Fermi level moves deeper in energy and now it falls within the gap and the total spin moment reaches the ideal value of 6 μ_B. So if Co_2MnAs can be grown on top of a substrate with the appropriate lattice constant using a technique like Molecular Beam Epitaxy, it is possible to get a material with a total spin moment of 6 μ_B. From the trends of Co_2MnSb and Co_2MnAs, I expect that Co_2MnP, if it exists, should have a total moment of 6 μ_B.

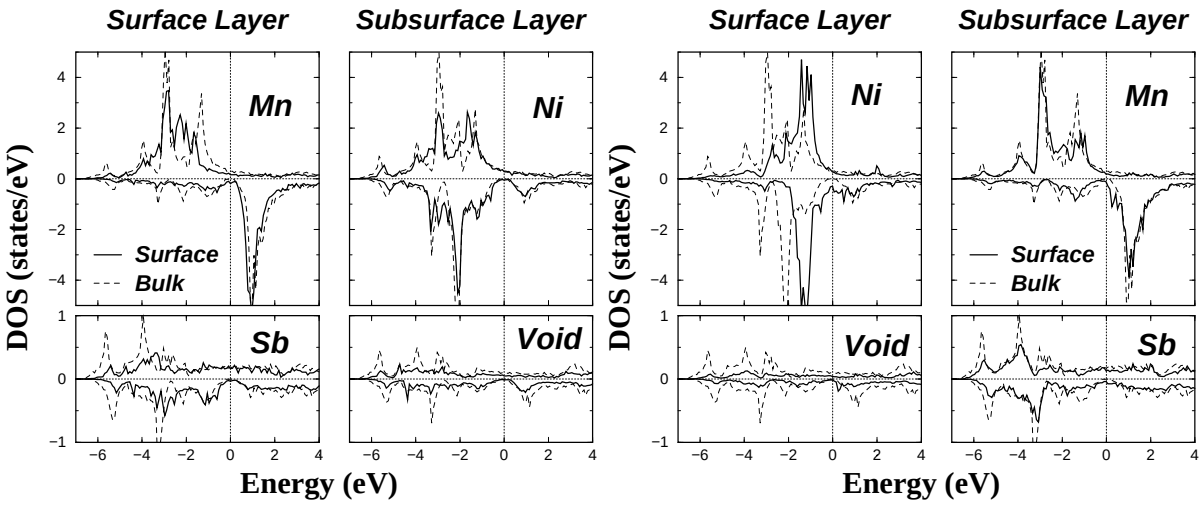

Figure 9. Spin- and atom-projected DOS for the MnSb-terminated NiMnSb(001) surface (left panel) and for the Ni-Void terminated (001) surface (right panel). The dashed lines give the local DOS of the atoms in the bulk.

5. Properties of the (001) Surfaces

5.1 Half-Heusler Alloys

In the first part of this section I concentrate on the half-Heusler compounds. I used the NiMnSb compound as the model system. As shown by Jenkins and King [31], the MnSb terminated surface of NiMnSb shows very small relaxations, while no information is available for the Ni-terminated surface which in principle should show large relaxations due to the vacant site at the surface. In my study I assume an "ideal" epitaxy in both cases. In the left panel of Fig. 9, I present the atom- and spin-projected density of states (DOS) for the Mn and Sb atoms in the surface layer and the Ni and vacant site in the subsurface layer for the MnSb terminated NiMnSb(001) surface, and in the right panel of the same figure I present the atom- and spin-projected DOS of the surface and the subsurface layers for the Ni terminated surface. In both cases I compare the surface DOS with the bulk calculations (dashed line).

In the case of the MnSb terminated surface the DOS with the exception of the gap area is very similar to the bulk calculations. The Ni atom in the subsurface layer presents practically a half-ferromagnetic character with an almost zero spin-down DOS, while for the bulk there is an absolute gap. The spin-down band of the vacant site also presents a very small DOS around the Fermi level. The Mn and Sb atoms in the surface layer show more pronounced differences with respect to the bulk, and within the gap there is a very small Mn-d and Sb-p DOS. These states are strongly localized at the surface layer as at the subsurface layer there is practically no states inside the gap. This is in agreement with previous pseudopotentials calculations that showed that the surface states at the case of the MnSb-terminated NiMnSb(001) surface are localized at the surface layer [31]. Our results are in agreement with the experiments of Ristoiu *et al.* [24] who in the case of a MnSb well ordered (001) surface measured a high spin-polarization.

It is also interesting to examine the spin-polarization at the Fermi level. In Table 2 we have gathered the number of spin-up and spin-down states at the Fermi level for each atom at the surface and the subsurface layer for both terminations. I calculated the spin-polarization as the ratio between the number of spin-up states minus the number of spin-down states over the total DOS at the Fermi level. P_1 corresponds to the spin-polarization when I take into account only the surface layer and P_2 when I also include the subsurface layer. P_2 represents quite well the experimental situation as the spin-polarization in the case of films is usually measured by inverse photoemission which probes only the surface of the sample [66]. In all cases the inclusion of the subsurface layer increased the spin-polarization. In the case of the Ni terminated surface, the spin-up DOS at the Fermi level is equal to the spin-down DOS and the net polarization P_2 is zero. In the case of the MnSb terminated surface the spin-polarization increases and now P_2 reaches a value of 38%, which means that the spin-up DOS at the Fermi level is about two times the spin-down DOS. As can be seen in Table 2 the main difference between the two different terminations is the contribution of the Ni spin-down states. In the case of the MnSb surface the Ni in the subsurface layer has a spin-down DOS at the Fermi level of 0.05 states/eV, while in the case of the Ni-terminated surface the Ni spin-down DOS at the Fermi level is 0.40 states/eV decreasing considerably the spin-polarization for the Ni terminated surface; the Ni spin-up DOS is the same for both terminations. It is interesting also to note that for both surfaces the net Mn spin-polarization is close to zero while Sb atoms in both cases show a large spin-polarization and the number of the Sb spin-up states is similar to the number of Mn spin-up states, thus Sb and not Mn is responsible for the large spin-polarization of the MnSb layer in

both surface terminations. The calculated P_2 value of 38% for the MnSb terminated surface is smaller than the experimental value of 67% obtained by Ristoiu and collaborators [24] for a thin-film terminated in a MnSb stoichiometric alloy surface layer. But experimentally no exact details of the structure of the film are known and the comparison between experiment and theory is not straightforward.

The other half-Heusler alloys present surface properties similar to the ones of NiMnSb. In the case of the Co terminated CoMnSb surface as it was the case for the Ni terminated surface there is a shift of the Co spin-down DOS towards higher energies and the Co spin-down DOS at the Fermi level is very high and thus P_2 is negative, meaning that the spin-down DOS is larger than the spin-up DOS at the Fermi level. In the case of the MnSb terminated CoMnSb surface, the Co atom in the subsurface layer has practically zero spin-down DOS and P_2 reaches 46%. In the case of PtMnSb, Pt does not show such a pronounced difference between the two surface terminations as the Co atom because it has practically all its d states filled and the DOS near the Fermi level is small. But also for PtMnSb the MnSb terminated surface shows a very large spin-polarization comparable to the one of CoMnSb, while the Pt terminated (001) surface shows a positive spin-polarization contrary to the vanishing net spin-polarization of the Ni surface and the negative one of the Co terminated surface.

Table 2. Atomic-resolved spin-up and spin-down DOS at the Fermi level in states/eV units. They are presented as ratios spin-up over spin-down. Polarization ratios at the Fermi level are calculated taking into account only the surface layer P_1, and both the surface and subsurface layers P_2.

	MnSb-termination					
	Surface Layer		Subsurface Layer			
	Mn ($\uparrow$ / $\downarrow$)	Sb ($\uparrow$ / $\downarrow$)	Ni[Co,Pt] ($\uparrow$ / $\downarrow$)	Void ($\uparrow$ / $\downarrow$)	P_1 ($\frac{\uparrow-\downarrow}{\uparrow+\downarrow}$)	P_2 ($\frac{\uparrow-\downarrow}{\uparrow+\downarrow}$)
NiMnSb	0.16/0.19	0.17/0.03	0.28/0.05	0.05/0.02	26%	38%
CoMnSb	0.23/0.27	0.16/0.07	0.91/0.15	0.07/0.02	6%	46%
PtMnSb	0.21/0.24	0.31/0.06	0.38/0.04	0.08/0.02	26%	46%
	Ni(Co,Pt)Void-termination					
	Subsurface Layer		Surface Layer			
	Mn ($\uparrow$ / $\downarrow$)	Sb ($\uparrow$ / $\downarrow$)	Ni[Co,Pt] ($\uparrow$ / $\downarrow$)	Void ($\uparrow$ / $\downarrow$)	P_1 ($\frac{\uparrow-\downarrow}{\uparrow+\downarrow}$)	P_2 ($\frac{\uparrow-\downarrow}{\uparrow+\downarrow}$)
NiMnSb	0.18/0.16	0.13/0.05	0.27/0.40	0.04/0.02	-16%	0%
CoMnSb	0.55/0.68	0.12/0.07	0.54/1.15	0.05/0.04	-34%	-22%
PtMnSb	0.18/0.14	0.21/0.07	0.30/0.24	0.05/0.02	14%	22%

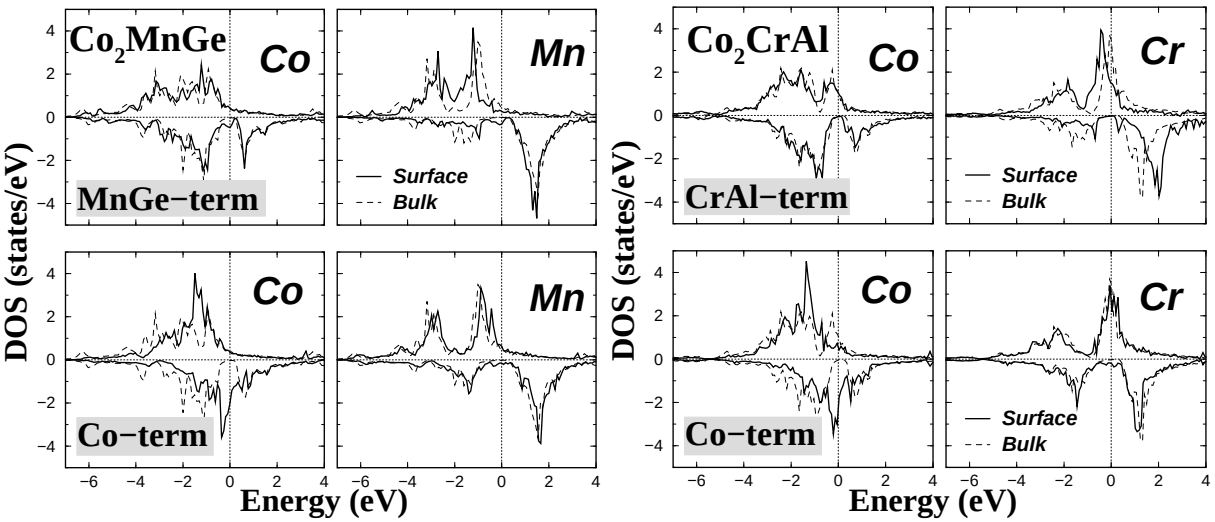

Figure 10. Atom- and spin-projected DOS for the Mn atom in the surface and the Co atom in the subsurface layer in the case of the MnGe terminated Co_2MnGe (001) surface (left upper panel) and the Co atom in the surface layer and the Mn atom in the subsurface for the Co terminated surface (left bottom panel). In the right panel similar DOS for the Co_2CrAl compound. With dashed line the bulk results.

5.2 Full-Heusler Alloys

I continue my study with the full-Heusler alloys and concentrate mainly on the Co_2MnGe, Co_2MnSi and Co_2CrAl alloys. Co_2MnGe and Co_2MnSi present similar surface properties and thus I will discuss in detail only the properties of Co_2MnGe. As shown in Fig. 10, in the case of the Co terminated surfaces all compounds show the same behavior which is similar to the behavior of the Co surface atom in the case of the Co-terminated CoMnSb surface. The lower coordination number of the Co atoms in the surface layer results in smaller covalent hybridization between the Co spin-down d states and the Mn ones and thus there is a practically rigid shift of the spin-down Co d bands towards higher energies, and now the Fermi level falls at the edge of the large peak of the minority spin DOS.

In the case of the MnGe terminated Co_2MnGe (001) surface the behavior is similar to the MnSb terminated surface in the CoMnSb compound. Due to the reduced symmetry (Mn loses two out of the four Co nearest neighbors) the hybridization between the Mn minority d states and the Co ones is reduced, leading to an increase of the Mn spin-moment by about 0.6 μ_B, while the Co atom at the subsurface layer behaves similar to the bulk case. Where the Mn gap was located in the bulk, there is now a small peak due to a d like Mn atomic state that is shifted in energy due to the lower symmetry and which is pinned at the Fermi level. This state although located at the surface layer is not well localized and the Co atoms in the subsurface layer present a similar peak at the Fermi level. Ishida *et al.* [41] have studied the MnSi and MnGe terminated Co_2MnSi and Co_2MnGe surfaces using a 13 layers thick film. They claim that in the case of the MnSi surface the half-ferromagnetic character, which they have calculated for the bulk Co_2MnSi [36], is preserved, while in the case of the MnGe surface, surface states destroy the gap (in the

paper they present the results for the MnSi surface and only shortly refer to the MnGe surface). These results are peculiar since they get a similar electronic structure for the bulk compounds and there is no obvious reason obliging only the MnGe surface to present surface states. Mn atoms have the same environment in both cases and the hybridization between Mn and the *sp* atoms is similar for both Ge and Si. A plausible reason for this behavior is the use of the atomic-sphere approximation in their calculations, where the potential and the charge density are supposed to be spherically symmetric. Although this approximation can accurately describe the bulk compounds due to the close-packed structure they adopt, it is not suitable for surfaces where the non-spherical contributions to the potential and the charge density are important.

The case of Co_2CrAl is different from Co_2MnGe. In line with the reduction of the total valence electrons by 2, the Cr moment is rather small (1.54 μ_B) yielding a total moment of only 3 μ_B instead of 5 μ_B for Co_2MnGe. The Co terminated $Co_2CrAl(001)$ surface shows a similar behavior as the corresponding surface of Co_2MnGe, being in both cases dominated by a strong Co peak in the gap region of the minority band. However the CrAl terminated Co_2CrAl surface behaves very differently, being driven by the large surface enhancement of the Cr moment from 1.54 μ_B to 3.12 μ_B. As a consequence the splitting of the Cr peaks in the majority and minority bands is even enlarged and in particular in the minority band the pseudogap is preserved. Thus this surface is a rare case, since for all the other surfaces studied in this paper, the half-metallicity is destroyed by surface states.

In the last part of this section I will discuss the spin-polarization for the surfaces of the full-Heusler alloys. We concentrate on the MnGe and CrAl terminated surfaces as the Co-terminated ones might show large relaxation and thus are not interesting for applications. In Fig. 11, I present the DOS for the atoms in the surface and subsurface layers for both surfaces. In the case of the MnGe terminated surface the surface states completely kill the spin polarization as the majority spin DOS is pretty small. In the case of the CrAl terminated surface the situation is completely different. The minority DOS around the Fermi level is the same for both the bulk and the CrAl surface. Only Al atoms posses surface states. The Fermi level falls within a region of very high Cr and Co majority spin DOS reducing the effect of these surface states and thus 92% of the electrons at the Fermi level are of spin-up character and the surface keeps a high degree of spin-polarization; P_2 reaches 84%.

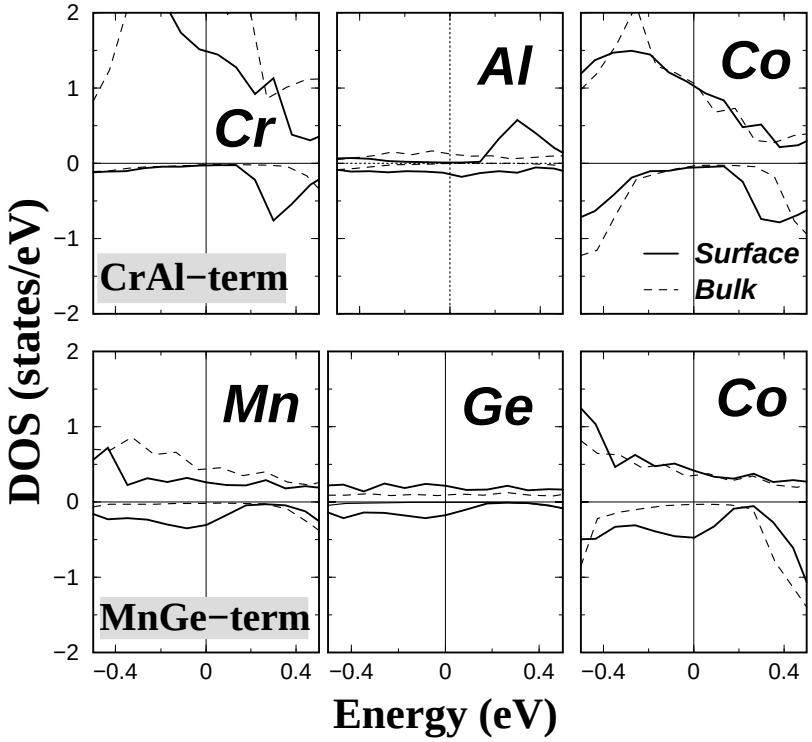

Figure 11. Atom- and spin-projected DOS for the MnGe and CrAl terminated (001) surfaces of Co_2MnGe and Co_2CrAl, respectively. With dashed line: the bulk results.

6. CrAs in the zinc-blende structure

Akinaga and collaborators have managed to grow thin films of CrAs on GaAs(100) substrates by molecular-beam epitaxy [10]. They have found that CrAs is ferromagnetic at room temperature with a T_c larger than 400 K and they have deduced a total spin-magnetic moment of 3 μ_B. Bulk CrAs adopts either the MnP-type structure showing a helimagnetic-paramagnetic transition at 256 K, or it crystallizes as Cr_2As which is an antiferromagnet with a Néel temperature of 393 K. So the structure of the thin film cannot be one of the two stable bulk structures. Akinaga *et al.* have made the assumption that CrAs adopts the zinc-blende (zb) structure of GaAs and using the full-potential linearized augmented-plane-wave (FLAPW) method they have shown that in the ferromagnetic case zb-CrAs would be a half-metal with a total spin magnetic moment of 3 μ_B in agreement with the experiment. Afterwards, Shirai [67] continued the theoretical study of the 3*d*-transitional monoarsenides and showed that the half-ferromagnetic phase for zb-CrAs should be more stable than the antiferromagnetic solution. He also calculated the theoretical equilibrium lattice constant and found a value of 0.58nm, which lies inbetween the experimental lattice constants of GaAs (0.565nm), AlAs (0.566nm) and InAs (0.606nm).

Using the FSKKR I verified that bulk CrAs is a half-ferromagnet with a total spin moment of 3 μ_B for both the GaAs and InAs lattice constants. The explanation of why there are exactly 3 uncompensated spin states is similar to the one for the half-ferromagnetic Heusler alloys. The As atom in the minority band offers one s band and three p bands low in energy and

can accommodate 4 electrons. There are practically no occupied minority d states. The total number of uncompensated spins should be just the total number of valence electrons, 11, minus two times the number of occupied minority states, 2×4=8, and the total spin moment in μ_B would be also (11−8) μ_B= 3 μ_B.

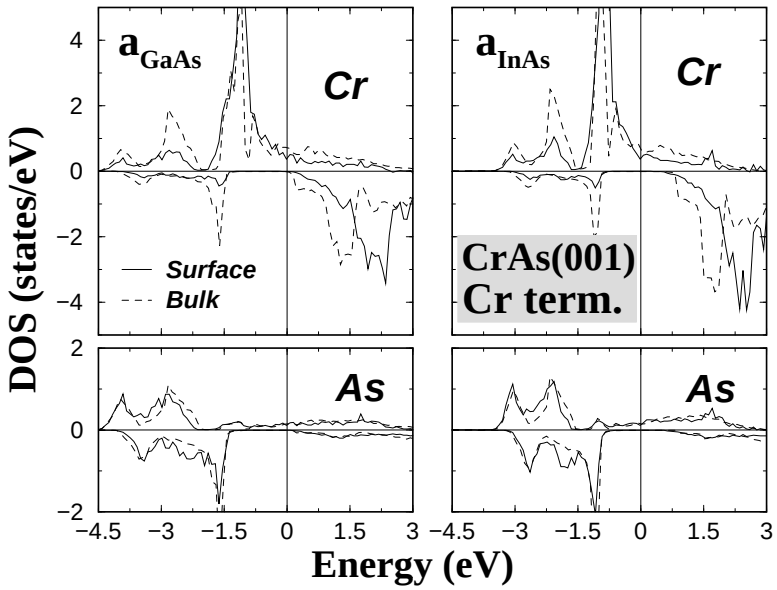

Figure 12. Spin- and atom-resolved DOS of the Cr-terminated (001) surface for the Cr atom at the surface layer and the As atom at the subsurface layer for both the GaAs and InAs lattice constants. The surface DOS are compared to the bulk calculations (dashed lines).

I have also studied the (001) surfaces of CrAs taking into account both the Cr- and As-terminations. I present in Fig. 12 the atomic projected DOS for the Cr atom at the surface and the As atom at the subsurface layer for the Cr-terminated surface and for both the GaAs and InAs lattice constants. There are no surface states within the gap, so this surface is half-ferromagnetic. To our knowledge this is the first case that electronic structure calculations predict a surface of an intermetallic compound to present 100% spin-polarization at the Fermi level. The As-atom at the subsurface layer has the same tetrahedral environment as in the bulk and the amount of electronic charge, which it looses, is similar to the bulk case. However the DOS of the Cr surface is very different, since the unoccupied Cr minority is shifted to higher energies and the Cr admixture in the occupied part of the minority band is decreased. Thus, while the hybridization with the missing As neighbors should decrease the Cr minority peak, this is overcompensated by the increase of the Cr moment by 0.95 μ_B, which shift the Cr peak to higher energies and stabilizes the gap. The same effect is responsible for the high spin-polarization of the CrAl-terminated $Co_2CrAl(001)$ surface (Fig. 10). The conservation of the half-metallic character at the Cr-terminated CrAs(001) surface means that the total moment increases due to the creation of the surface by exactly 1 μ_B.

In the case of the As-terminated (001) surface the situation is not as ideal as in the case of the Cr terminated surface. Now the As dangling bonds create a surface band within the gap that destroys the half-ferromagnetic character. In the case of the InAs lattice constant the gap is only partially destroyed but the Fermi level is below the remaining fully spin-polarized region. Contrary to the Cr-termination the DOS of both the As surface atom and the Cr subsurface atom present large deviations from the bulk case. The As atom at the surface looses ~ 0.4 more electrons than in the bulk CrAs. Its spin magnetic moment is practically doubled. Although the Cr atoms at the subsurface layer present a charge transfer comparable to the bulk calculations, the changes in their DOS are pronounced, the spin imbalance decreases and their magnetic moment is 0.3-0.4 μ_B lower than in the bulk CrAs.

7. Summary

Using the full-potential screened KKR method I studied the bulk and surface properties of both the half and full Heusler alloys identifying a total of 30 half-ferromagnetic compounds. I have shown that in the case of the half-Heusler alloys with 18 valence electrons, like CoTiSb, the d states of Co and Ti hybridize forming ten bonding and ten antibonding states. The large covalent hybridization results in a gap between the occupied and the unoccupied states and the Fermi level falls within this gap. The Sb atom creates two s and six p bands low in energy which accommodate d transition metal electrons (Sb atom acts like an anion: Sb^{-3}) reducing the effective valence d charge, which can now be accommodated only in the bonding d states and CoTiSb is a semiconductor. This behavior of Sb is general for all the sp atoms and it is found even when Sb is replaced by Al; in this case the sp bands accommodate 5 transition metal d electrons and Al acts like an Al^{-5} ion. In the case of compounds with more than 18 electrons like NiMnSb the extra electrons are taken care only by the spin-up states and the minority bands stay unchanged. Thus there are nine occupied spin-down states and the total spin moment per unit cell (M_t) scales with the total number of valence electrons following the relation: $M_t = Z_t - 18$. This is similar to the well-known Slater-Pauling behavior observed for the transition metal binary alloys, except that in this case the total moment decreases with the total number of valence electrons. Thus the total spin moment of NiMnSb which has 22 valence electrons is calculated to be 4 μ_B, the one of CoMnSb (21 valence electrons) 3 μ_B and the spin moment of FeMnSb (20 valence electrons) 2 μ_B. The maximum moment of the half-Heusler alloys is 5 μ_B, since there are five unoccupied minority d-states, but this value is difficult to be achieved.

In the case of the full-Heusler alloys like Co_2MnGe, there are in addition to the Co-Mn bonding and antibonding d-hybrids, also Co states which cannot hybridize with neither the Mn nor the Ge atoms and are exclusively localized at the Co sites. Thus in addition to the 5 Co-Mn bonding and 5 Co-Mn antibonding states, there exist 5 such "non-bonding" states which are only splitted-up by the weaker Co-Co hybridization into 3 occupied d states of t_{1u} symmetry and 2 unoccupied e_u states, which are located just below and just above the Fermi level such that the indirect gap in these materials is tiny. These extra three electrons make that for the

full-Heusler alloys there are 12 occupied minority states instead of 9 in the case of the half-Heusler compounds and the relation for the total spin magnetic moment becomes $M_t = Z_t - 24$. Thus systems like Fe_2VAl with 24 valence electrons are semiconductors with a tiny gap, Co_2VAl (26 valence electrons) has a total spin moment of 2 μ_B, Co_2CrAl 3 μ_B, Co_2MnAl 4 μ_B and finally Co_2MnSi which has 29 valence electrons has a total spin moment of 5 μ_B. This law is also valid for compounds with less than 24 electrons, *e.g* Mn_2VGe and Mn_2VAl which have 23 and 22 valence electrons, respectively, have total moments of -1 and -2 μ_B. The maximal total spin moment for these alloys is 7 μ_B, but as has been shown even the 6 μ_B are unlikely to be achieved.

The surfaces of the Heusler alloys in general loose the half-ferromagnetic character of the bulk compounds. The lower coordination of the atoms at the surface leads to a decrease of the hybridization in the minority band resulting in surface states within the gap, which practically kill the high spin-polarization. However the effect of surfaces states can be reduced by the increase of the local moment of the atoms at the surface. Such an example is the CrAl-terminated $Co_2CrAl(001)$ surface where the Cr moment increases from the bulk value of 1.5 μ_B to more than 3 μ_B and the very large spin-up density of states of the Cr atoms at the surface leads to a spin-polarization of 84%. In the case of the Cr-terminated CrAs(001) the surface even retains the half-metallic character of the bulk CrAs in the metastable zinc-blende structure. Thus the large surface enhancement of the Cr atoms stabilizes the gap at the surface.

Acknowledgments

The author acknowledges financial support from the RT Network of *Computational Magneto-electronics* (contract RTN1-1999-00145) of the European Commission.

References

[1] F. Heusler, Verh. Dtsch. Phys. Ges. **5**, 219 (1903).

[2] P.J. Webster and K.R.A. Ziebeck, in *Alloys and Compounds of d-Elements with Main Group Elements. Part 2.*, edited by H.R.J. Wijn, Landolt-Boörnstein, New Series, Group III, Vol. 19/c (Springer, Berlin), 1988, pp. 75-184.

[3] K.R.A. Ziebeck and K.-U. Neumann, in *Magnetic Properties of Metals*, edited by H.R.J. Wijn, Landolt-Boörnstein, New Series, Group III, Vol. 32/c (Springer, Berlin), 2001, pp. 64-414.

[4] J. Pierre, R.V. Skolozdra, J. Tobola, S. Kaprzyk, C. Hordequin, M.A. Kouacou, I. Karla, R. Currat, and E. Lelièvre-Berna, J. Alloys Comp. **262-263**, 101 (1997).

[5] J. Tobola and J. Pierre, J. Alloys Comp. **296**, 243 (2000).

[6] R.A. de Groot. F.M. Mueller, P.G. van Engen, and K.H.J. Buschow, Phys. Rev. Lett. **50**, 2024 (1983).

[7] S.A. Wolf, D.D. Awschalom, R.A. Buhrman, J.M. Daughton, S. von Molnár, M.L. Roukes, A.Y. Chtchelkanova, and D.M. Treger, Science **294**, 1488 (2001); G.A. Prinz, Science **282**, 1660 (1998); G.A. Prinz, J. Magn. Magn. Mater. **200**, 57 (1999).

[8] R.J. Soulen Jr., J.M. Byers, M.S. Osofsky, B. Nadgorny, T. Ambrose, S.F. Cheng, P.R. Broussard, C.T. Tanaka, J. Nowak, J.S. Moodera, A. Barry, and J.M.D. Coey, Science **282**, 85 (1998).

[9] H. Akai, Phys. Rev. Lett. **81**, 3002 (1998).

[10] H. Akinaga, T. Manago, and M. Shirai, Jpn. J. Appl. Phys. **39**, L1118 (2000).

[11] J.-H. Park, E. Vescovo, H.-J. Kim, C. Kwon, R. Ramesh, and T. Venkatesan, Nature **392**, 794 (1998).

[12] S. Datta and B. Das, Appl. Phys. Lett. **56**, 665 (1990).

[13] K.A. Kilian and R.H. Victora, J. Appl. Phys. **87**, 7064 (2000).

[14] C.T. Tanaka, J. Nowak, and J.S. Moodera, J. Appl. Phys. **86**, 6239 (1999).

[15] J.A. Caballero, Y.D. Park, J.R. Childress, J. Bass, W.-C. Chiang, A.C. Reilly, W.P. Pratt Jr., and F. Petroff, J. Vac. Sci. Technol. A **16**, 1801 (1998); C. Hordequin, J.P. Nozières, and J. Pierre. J. Magn. Magn. Mater. **183**, 225 (1998).

[16] M.M. Kirillova, A.A. Makhnev, E.I. Shreder, V.P. Dyakina, and N.B. Gorina, Phys. Stat. Sol. (b) **187**, 231 (1995).

[17] K.E.H.M. Hanssen and P.E. Mijnarends, Phys. Rev. B **34**, 5009 (1986); K.E.H.M. Hanssen, P.E. Mijnarends, L.P.L.M. Rabou, and K.H.J. Buschow, Phys. Rev. B **42**, 1533 (1990).

[18] W. van Roy, J. de Boeck, B. Brijs, and G. Borghs, Appl. Phys. Lett. **77**, 4190 (2000); J.-P. Schlomka, M. Tolan, and W. Press, Appl. Phys. Lett. **76**, 2005 (2000).

[19] F.B. Mancoff, B.M. Clemens, E.J. Singley, and D.N. Basov, Phys. Rev. B **60**, *R*12 565 (1999).

[20] W. Zhu, B. Sinkovic, E. Vescovo, C. Tanaka, and J.S. Moodera, Phys. Rev. B **64**, *R*060403 (2001).

[21] G.L. Bona, F. Meier, M. Taborelli, E. Bucher, and P.H. Schmidt, Sol. St. Commun. **56**, 391 (1985).

[22] J.A. Caballero, A.C. Reilly, Y. Hao, J. Bass, W.P. Pratt, F. Petroff, and J.R. Childress, J. Magn. Magn. Mat. **198-199**, 55 (1999); R. Kabani, M. Terada, A. Roshko, and J.S. Moodera, J. Appl. Phys. **67**, 4898 (1990).

[23] C.T. Tanaka, J. Nowak, and J.S. Moodera, J. Appl. Phys. **81**, 5515 (1997).

[24] D. Ristoiu, J.P. Nozières, C.N. Borca, T. Komesu, H.-K. Jeong, and P.A. Dowben, Europhys. Lett. **49**, 624 (2000); D. Ristoiu, J.P. Nozières, C.N. Borca, B. Borca, and P.A. Dowben, Appl. Phys. Lett. **76**, 2349 (2000); T. Komesu, C.N. Borca, H.-K. Jeong, P.A. Dowben, D. Ristoiu, J.P. Nozières, Sh. Stadler, and Y.U. Idzerda, Phys. Lett. A **273**, 245 (2000).

[25] C.N. Borca, T. Komesu, H.-K. Jeong, P.A. Dowben, D. Ristoiu, Ch. Hordequin, J.P. Nozières, J. Pierre, Sh. Stadler, and Y.U. Idzerda, Phys. Rev. B **64**, 052409 (2001).

[26] I. Galanakis, S. Ostanin, M. Alouani, H. Dreyssé, and J.M. Wills, Phys. Rev. B **61**, 4093 (2000).

[27] E. Kulatov and I.I. Mazin, J. Phys.: Condens. Matter **2**, 343 (1990); S.V. Halilov and E.T. Kulatov, J. Phys.: Condens. Matter **3**, 6363 (1991); X. Wang, V.P. Antropov, and B.N. Harmon, IEEE Trans. Magn. **30**, 4458 (1994). S.J. Youn and B.I. Min, Phys. Rev. B **51**, 10 436 (1995); V.N. Antonov, P.M. Oppeneer, A.N. Yaresko, A.Ya. Perlov, and T. Kraft, Phys. Rev. B **56**, 13 012 (1997).

[28] P. Larson, S.D. Mahanti, and M.G. Kanatzidis, Phys. Rev. B **62**, 12 574 (2000).

[29] D. Orgassa, H. Fujiwara, T.C. Schulthess, and W.H. Butler, Phys. Rev. B **60**, 13 237 (1999).

[30] G.A. Wijs and R.A. de Groot, Phys. Rev. B **64**, *R*020402 (2001).

[31] S.J. Jenkins and D.A. King, Surf. Sci. **494**, L793 (2001).

[32] S.J. Jenkins and D.A. King, Surf. Sci. **501**, L185 (2002).

[33] P.J. Webster, J. Phys. Chem. Solids **32**, 1221 (1971); K. R.A. Ziebeck and P.J. Webster, J. Phys. Chem. Solids **35**, 1 (1974).

[34] J.C. Suits, Phys. Rev. B **14**, 4131 (1976).

[35] J. Kübler, A.R. Williams, and C.B. Sommers, Phys. Rev. B **28**, 1745 (1983).

[36] S. Ishida, S. Akazawa, Y. Kubo, and J. Ishida, J. Phys. F: Met. Phys. **12**, 1111 (1982); S. Ishida, S. Fujii, S. Kashiwagi, and S. Asano, J. Phys. Soc. Jpn. **64**, 2152 (1995).

[37] S. Fujii, S. Sugimura, S. Ishida, and S. Asano, J. Phys.: Condens. Matter **2**, 8583 (1990).

[38] S. Fujii, S. Ishida, and S. Asano, J. Phys. Soc. Jpn. **64**, 185 (1995).

[39] P.J. Brown, K.U. Neumann, P.J. Webster, and K.R.A. Ziebeck, J. Phys.: Condens. Matter **12**, 1827 (2000).

[40] T. Ambrose, J.J. Krebs, and G.A. Prinz, Appl. Phys. Lett. **76**, 3280 (2000); T. Ambrose, J.J. Krebs, and G.A. Prinz, J. Appl. Phys. **87**, 5463 (2000).

[41] S. Ishida, T. Masaki, S. Fujii, and S. Asano, Physica B **245**, 1 (1998).

[42] U. Geiersbach, A. Bergmann, and K. Westerholt, J. Magn. Magn. Mater. **240**, 546 (2002).

[43] Half-Heusler alloys: I. Galanakis, P.H. Dederichs, and N. Papanikolaou, arXiv:cond-mat/0203534; Full-Heusler alloys: I. Galanakis, P.H. Dederichs, and N. Papanikolaou, arXiv:cond-mat/0205129; Surfaces of Heusler alloys: I. Galanakis, arXiv:cond-mat/0204083; CrAs: I. Galanakis, arXiv:cond-mat/0203535.

[44] S.H. Vosko, L. Wilk, and N. Nusair, Can. J. Phys. **58**, 1200 (1980).

[45] P, Hohenberg and W. Kohn, Phys. Rev. **136**, B864 (1964); W. Kohn and L.J. Sham, Phys. Rev. **140**, A1133 (1965).

[46] R. Zeller, P.H. Dederichs, B. Újfalussy, L. Szunyogh, and P. Weinberger Phys. Rev. B **52**, 8807 (1995).

[47] N. Papanikolaou, R. Zeller, and P.H. Dederichs, J. Phys.: Condens. Matter **14**, 2799 (2002).

[48] R. Zeller, Phys. Rev. B **55**, 9400 (1997); K. Wildberger, R. Zeller, and P.H. Dederichs, Phys. Rev. B **55**, 10074 (1997).

[49] R. Zeller, J. Deutz, and P.H. Dederichs, Sol. St. Comm. **44**. 993 (1982); K. Wildberger, P. Lang, R. Zeller, and P.H. Dederichs, Phys. Rev. B **52**, 11502 (1995).

[50] H.J. Monkhorst and J.D. Pack, Phys. Rev. B **13**, 5188 (1976).

[51] M.J. Otto, R.A.M. van Woerden, P.J. van der Valk, J. Wijngaard, C.F. van Bruggen, C. Haas, and K.H.J. Buschow, J. Phys.: Condens. Matter **1**, 2341 (1989); M.J. Otto, R.A.M. van Woerden, P.J. van der Valk, J. Wijngaard, C.F. van Bruggen, and C. Haas, J. Phys.: Condens. Matter **1**, 2351 (1989).

[52] J. Kübler, Physica B **127**, 257 (1984).

[53] M.V. Yablonskikh, V.I. Grebennikov, Yu.M. Yarmoshenko, E.Z. Kurmaev, S.M. Butorin, L.-C. Duda, C. Såthe, T. Kämbre, M. Magnuson, J. Nordgren, S. Plogmann, and M. Neumann, Solid State Commun. **117**, 79 (2001); M.V. Yablonskikh, Yu.M. Yarmoshenko, V.I. Grebennikov, E.Z. Kurmaev, S.M. Butorin, L.-C. Duda, J. Nordgren, S. Plogmann, and M. Neumann, Phys. Rev. B **63**, 235117 (2001).

[54] A. Kimura, S. Suga, T. Shishidou, S. Imada, T. Muro, S.Y. Park, T. Miyahara, T. Kaneko, T. Kanomata, Phys. Rev. B **56**, 6021 (1997).

[55] R.A. de Groot, A.M. van der Kraan, and K.H.J. Buschow, J. Magn. Magn. Mater. **61**, 330 (1986).

[56] D. Brown, M.D. Crapper, K.H. Bedwell, M.T. Butterfield, S.J. Guilfoyle, A.E.R. Malins, and M. Petty, Phys. Rev. B **57**, 1563 (1998).

[57] R.A. Dunlap and D.F. Jones, Phys. Rev. B **26**, 6013 (1982); S. Plogmann, T. Schlathölter, J. Braun, M. Neumann, Yu.M. Yarmoshenko, M.V. Yablonskikh, E.I. Shreder, E.Z. Kurmaev, A. Wrona, and A. Ślebarski, Phys. Rev. B **60**, 6428 (1999).

[58] D. Jung, H.-J. Koo, and M.-H. Whangbo, J. Mol. Struct. (Theochem) **527**, 113 (2000).

[59] J. Tobola, J. Pierre, S. Kaprzyk, R.V. Skolozdra, and M.A. Kouacou, J. Phys.: Condens. Matter **10**, 1013 (1998).

[60] L.P. Bouckaert, R. Smoluchowski, and E. Wigner, Phys. Rev. **50**, 58 (1936).

[61] P.G. van Engen, K.H.J. Buschow, and M. Erman, J. Magn. Magn. Mater. **30**, 374 (1983).

[62] W. Pendl Jr., R.N. Saxena, A.W. Carbonari, J. Mestnik Filho, and J. Schaff, J. Phys.: Condens. Matter **8**, 11317 (1996).

[63] Ye Feng, J.Y. Rhee, T.A. Wiener, D.W. Lynch, B.E. Hubbard, A.J. Sievers, D.L. Schlagel, T.A. Lograsson, and L.L. Miller, Phys. Rev. B **63**, 165109 (2001); C.S. Lue, J.H. Ross Jr., K.D.D. Rathnayaka, D.G. Naugle, S.Y. Wu and W.-H. Li, J. Phys.: Condens. Matter **13**, 1585 (2001); Y. Nishino, H. Kato, M. Kato, U. Mizutani, Phys. Rev. B **63**, 233303 (2001); A. Matsushita, T. Naka, Y. Takanao, T. Takeuchi, T. Shishido, and Y. Yamada, Phys. Rev. B **65**, 075204 (2002).

[64] T. Kanomata, M. Kikuchi, H. Yamauchi, and T. Kaneko, Jpn. J. Appl. Phys. **32** Suppl **32-33**, 292 (1993); M. Gotoh, M. Phashi, T. Kanomata, and Y. Yamaguchi, Physica B **213&214**, 306 (1995); S. Ishida, S. Kashiwagi, S. Fujii, and S. Asano, Physica B **210**, 140 (1995); .M. Pugacheva and A. Jezierski, J. Magn. Magn. Mater. **151**, 202 (1995)

[65] S. Jha, H.M. Seyoun, G.M. Julian, R.A. Dunlap, A. Vasquez, J.G.M. da Cunha, and S.M.M. Ramos, Phys. Rev. B **32**, 3279 (1985).

[66] C.N. Borca, T. Komesu, and P.A. Dowben, J. Electron Spectrosc. Relat. Phenom. **122**, 259 (2002).

[67] M. Shirai, Physica E **10**, 143 (2001).